Bull. Spec. Astrophys. Obs., 1996, 39, 47–58

UBV photometry of the Seyfert galaxy Mkn 1040

N. N. Pavlova[a], A. I. Shapovalova[b], F. Börngen[c], Ts. B. Georgiev[d]

[a] Astronomical Institute, Alma-Ata 68 Kamenskoe Plato, Kazakhstan
[b] Special Astrophysical Observatory of the Russian AS, Nizhnij Arkhyz 357147, Russia
[c] Karl-Schwarzschild Observatorium, Tautenburg 6901, Germany
[d] Rozhen National Observatory, BG-4700 Smolyan, Bulgaria

Received January 31, 1995; accepted February 10, 1995.

Abstract. Results are presented of UBV surface photometry of the Seyfert galaxy Mkn 1040: half–tone, isophote and isocolour maps, brightness profiles and distribution of U–B, B–V colours along the major and minor axes. Basic photometric parameters: concentration indices and integral properties of the host galaxy and companion are determined. Within the framework of a standard model decomposition into components is performed. The central lens is better described by the bright steep exponential disk $D1$ with a scale length of 1.27 kpc and $B(0)c = 19.9\,mag\,arcsec^{-2}$. The standard disk $D0$ is very extended, its parameters are 8.16 kpc, $B(0)c = 21.36\,mag\,arcsec^{-2}$, it is somewhat brighter than the Freeman disk. Their luminosity ratio is $D1/D0 = 0.11$, and the contribution to the integral luminosity of the thread–like spiral arms is about 2%. Comparison of the photometry results with the rotation curve yields the mass/luminosity ratio for the galaxy as a whole $M/L = 4.0$, for $D1$ $M/L = 6.8$, for $D0$ $M/L = 3.9$, $L_T = 8.2{\cdot}10^{10}L_\odot$, $M_T = 3.25{\cdot}10^{11}M_\odot$.

Key words: galaxies: Seyfert: individual: Mkn 1040 – UBV photometry

1. Introduction

Seyfert galaxies (Sy G) are very attractive to researchers not only due to the exotic properties of the active nuclei, but also due to their genetic link to quasars. Mostly the active nucleus is studied in isolation from the global properties of the host galaxy. However, for an active nucleus to originate and be fueled, probably particular conditions in the host galaxy itself are required. So far there is no clear answer to the question if AGN is a life stage of any galaxy, and the time of its activity is of the order of 10^8 years, or AGN originates only in galaxies with specific physical and dynamical features and live as long as the life time of the galaxy itself, $10^{10} - 10^{11}$ years. Morphological, statistical and photometric investigations (Adams, 1977; Simkin et al., 1980; Pavlova, 1981; Malkan et al., 1984; Dahary and Robertis, 1988; MacKenty, 1990, Yee, 1983; Xanthopoulos and Robertis, 1991; Kotilainen et al., 1993) point out to such morphological features of Sy G as bright star–like nuclei, larger number of bars, rings, various jets and ejections, distortions perturbations, which suggest possible interaction in the past; the presence of three–step structures with extended outer rings and thin spiral arms, which testify to an extended flat disk with a very flattened drop of luminosity, or, on the contrary, to concentration of radiation in a powerful central body with the apparent absence of outer envelopes. The presence of Sy G in small groups and among interacting galaxies is increased, although they avoid rich clusters. There are examples of double nuclei. One of the most popular hypotheses about the origin of the AGN is that the nuclear activity is triggered by interaction which turbulates gas in the galaxy and injects it into the centre. However there are quite a few examples of single Seyfert galaxies without apparent signs of disturbance. Investigation of circumnuclear regions and comparison of their properties in Seyfert and normal galaxies (NG) may provide answers to some questions about the origin of the AGN and its interaction with the host galaxy. Such a relationship between the active nucleus and external structures has been revealed in some Sy G as giantic superassociations of young clusters and gas (Metik and Pronik, 1981). The circumnuclear regions of Sy G and NG show noticeable differences. On the two–colour diagram Sy G are mostly situated on one side of the normal sequence. Both the blue colour excess, which is likely to be associated with the high intensity of star formation, and the anomalously red colour, B–V$\geq 1^m.1$ for many Sy G are characteristic of them, which is not typical even of elliptical galaxies and can not be accounted for by the selective absorption (Zasov and Neizvestny, 1989). Afanasiev (1981) has obtained rotation curves of about 20 Sy G and discovered that in most of them local maxima are

present, which suggest the existence of subsystems rotating at different radial velocities. The obtained integral masses of Seyfert galaxies do not differ from masses of normal galaxies (NG). However the mass-to-luminosity ratio in Sy G ($M/L = 4$) is considerably less than in normal spirals of the same morphological type. According to Afanasiev (1990) in Sy G one observes either a more extended and slower rotating disk, as compared to NG, or a powerful concentrated buldge with a normally rotating disk. That is why for a galaxy to have an active nucleus, a definite relation between the depth of the potential well in the centre and the specific moment of gas is required. Thus, to understand the nature of nuclear activity, it is necessary to continue the search for parameters by which Seyfert galaxies differ from normal. We are planning a detailed photometric study of a number of Seyfert galaxies in some colour bands and comparison of the photometry results with the dynamical parameters, where it is possible, to reveal the peculiarities of the host galaxy. In this paper we present the UBV-photometry results for Sy1 Mkn 1040.

2. Information about Mkn 1040

Mkn 1040 (Fig.1) posseses many morphological features characteristic of Sy G: three-step structure, very extended flat disk, its integral diameter is 84 kpc at the level 26 $mag\,arcsec^{-2}$. Its rotation curve has a local maximum at $R = 4.8$ kpc, minimum at 8 kpc, and a long plateau up to 25 kpc (Afanasiev, 1981). Mkn 1040 has a companion perturbed by tidal interaction. The catalogue of Seyfert galaxies (Lipovetsky et al., 1987) contains the following information about this galaxy: Sy1, SAbc, $cz_0 = 4920$ km/s, $B_T = 13\overset{m}{.}67$, U-B=0.34, B-V=0.89, $M_B = -20\overset{m}{.}73$. MacKenty (1990) provides for the galaxy an exponential disk scale length of 10.88 kpc in the V band. For the B band Afanasiev (1990) has obtained its value of 7.6 kpc at $H = 75 km/s/Mpc$. Rafanelli, Schulz (1983) consider it Sy 1.2 with a mini-quasar at the centre, which has $M_v = -16\overset{m}{.}85$ and anomalously high content of dust surrounding the nucleus. For this galaxy $I_{FIR} = 51 I_\odot$, $L(60)/L(100) = 0.58$.

On our plates a very small star-like nucleus with $R = 2''$ can be seen, which is located in the dusty lens. In the latter two thin clearly outlined spiral arms start, which are developed by 2.5–3 revolutions. The disk of the galaxy is dusty as well. The powerful dust lanes which are situated on the inside of the spirals are fairly distinguishable. Along the diameter ($183'' = 58$ kpc) one can see H_α emissions which coincide with bright knots in the spiral arms. These are likely to be giantic HII regions. The brightest H_α emission knots are located at a distance of $15''$ from the centre inside the lens at the intersection by the line of nodes of the first turn of the spiral arm where the local maximum

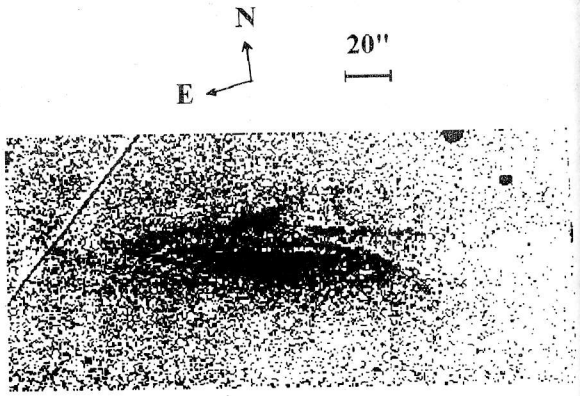

Figure 1: *The photograph of Mkn 1040 in the B filter (taken by A.I. Shapovalova at the 6 m telescope).*

of the rotation curve is located (Afanasiev, 1990). The companion of Mkn 1040 is situated $19''$ north of the galactic nucleus. Behind the companion in the north a very faint spiral arm, looking like separate low contrast brightenings, is discernable. The galactic plane is strongly inclined to the line of sight. From the outermost isophotes $b/a = 0.29$, which yields an inclination angle $i = 73°$. The proper absorption of the galaxy amounts then to $A_B = 0\overset{m}{.}68$, E(B-V)$=0\overset{m}{.}15$, E(U-B)$=0\overset{m}{.}12$.

3. Observations and data reduction

Photographs of the galaxy NGC 1040 at U,B,V filtres were taken during the autumn runs from 1977 through 1979 at the Tautenburg Observatory at the prime focus of the 2 m Schmidt telescope (the scale is $51''.7/mm$). Two or three plates were taken in each colour with different exposures for confident photometry of both the central region and the faint outer regions of the galaxy. The observations were conducted only on photometric nights. Immediately after the exposure a photometric wedge was exposed at the edge of each plate. Following the galaxy, off-focus photographs of the galactic cluster NGC 188 were obtained, using the same exposure. It was suggested that the stars of this cluster should be used for plotting characteristic curves. In the process of data reduction we saw that the photometric wedge allowed a sufficient accuracy in plotting characteristic curves. At the same time the use of the NGC 188 stars for this purpose in the case of long exposure time produced large errors. This was associated with the situation that due to the high density of the stars their off-focus images were frequently superimposed on each other. The instrumental colour system was investigated using the stars of this cluster. It was shown that this system is consistent with the Johnson

standard UBV system with an accuracy of $\pm 0^{m}.03$.

Images of the galaxy in AMD densities were recorded on a magnetic tape on the microdensitometer AMD1 of SAO RAS with a square aperture of $30 \times 30 \mu m$, corresponding to $1''.53 \times 1''.53$, and a step of $20 \mu m = 1''.02$. The dynamic range of the AMD is from 0 to $4D$, the AMD noise is much lower than the photographic emulsion noise. A rectangular region of 1.5–2 galactic diameters in size would usually be scanned to reliably define the sky background. The object would be positioned at the frame's centre, the zero point of the recorded image would be set by some faint star near the galaxy being scanned. When different frames of the same object are made coincident a displacement of 1 pixel ($1''.02$) is possible. Orientation of the frame being recorded was performed by two reference stars selected along the major axis of the galaxy. Following the image recording, the photometric wedge of each plate was recorded under the same conditions and with the same measuring diaphragm. The stars of NGC 188 were measured in the same manner.

Subsequent reduction of digital images was carried out at SAO RAS on a mini–computer with a graphical station ROBOTRON. Upon so doing a colour graphical display with 8–bite frames of 512×512 pixels was used. The image visualization and adaptive smoothing were made with the help of the Babelsberg input software (Richter and Lorenz, 1989). All the procedures of photometric reduction were accomplished using the Rozhen software (Georgiev, 1990). The photometric reduction included the procedures of filtering, smoothing and, if necessary, background balancing, the definition of the frame shift with respect to each other, their merging and averaging, and also the removal of interfering background stars and galaxies. The noise of the Tautenburg plates appeared to be uniform enough, therefore there was no need in background balancing. The smoothing was done by the method of adaptive filtering (Richter, 1978). The procedure of linearized imaging comprises the construction of a characteristic curve, using the photometric wedge records for each plate, and determination parameters of its approximating function in the form:

$$lgI = c_0 + c_1 D + c_2 D^2 + c_3 D^3 + c_4 lgD + c_5 e^D.$$

Next the image in densities $D(x, y)$ was converted to relative intensities $I(x, y)$. The linearized images were compared with one another to check for the displacement and turn of the frames with respect to each other. In all cases the displacements did not exceed 1 pixel. The orientation of frames was also good, therefore no coordinate correction was needed. Only after such coordinate check the linearized images in one colour were averaged. After that the linearized images were converted to magnitudes per square second of arc with the help of the aperture calibration program. Absolute calibrations of the images were performed using the photometric measuremens of Neizvestny (1986). It is as if the program simulated the performance of the electrophotometer. In the specified circular areas mean values of the digital photographic image are computed. Next, from their comparison and subtraction from one another over all diaphragms the values of the sky background level and the standardizing constant are defined. Here one can exclude the diaphragms which yield excessively different values of the constants. With the parameters thus calculated magnitudes of the galaxy in the corresponding diaphragms are determined from both each plate and averaged images. Comparison of these values with one another and with the photoelectric data allows us to judge of the accuracy of photometry. In absolute calibrations the data for circular diaphragms with diameters less than $6''$ were not used in order to rule out the nuclear effect which may be variable in Sy G. Besides because of the overexposures and high surface brightness gradients, the calibrations in this region appear to be not reliable enough. The results of integral photometry over different plates in one colour are in good agreement with one another, the spread does not exceed $0^{m}.05$. However, comparison with the photoelectric data points out to our systematic underestimation of brightness of the nuclear region. In the central diaphragm ($d \leq 2''.5$) the obtained brightnesses prove to be lower than the photoelectric estimates by more than 1^{m}. This is mainly due to the following: 1) nucleus AMD densities correspond to the region of overexposures on the characteristic curve, 2) scatter of light by photographic emulsion (its characteristic scale is $30 \mu m$), 3) the procedure of smoothing somewhat blurs the nucleus, decreasing artificially its surface brightness.

4. Photometry results

4.1. Maps of brightness and colour distribution

The resulting calibrated images in magnitudes per square second of arc are output in the form of both half–tone maps with tone gradation every $0^{m}.2$ and isophote maps at intervals of $0^{m}.5$ (Figs.2–4). Besides, isocolour maps were obtained in U–B and B–V colours (Fig.5). Brightness and colour index profiles along the minor and major axes are also presented (Figs.6,7). Comparison with the photoelectric data yields for the brightness and U–B, B–V index profiles rms errors $0.05\, mag\, arcsec^{-2}$, $0^{m}.1$ and $0^{m}.2$ for one element, respectively. Colour details on the maps have sizes of tens of pixels, therefore the light variation appear to be real. These maps give an idea of

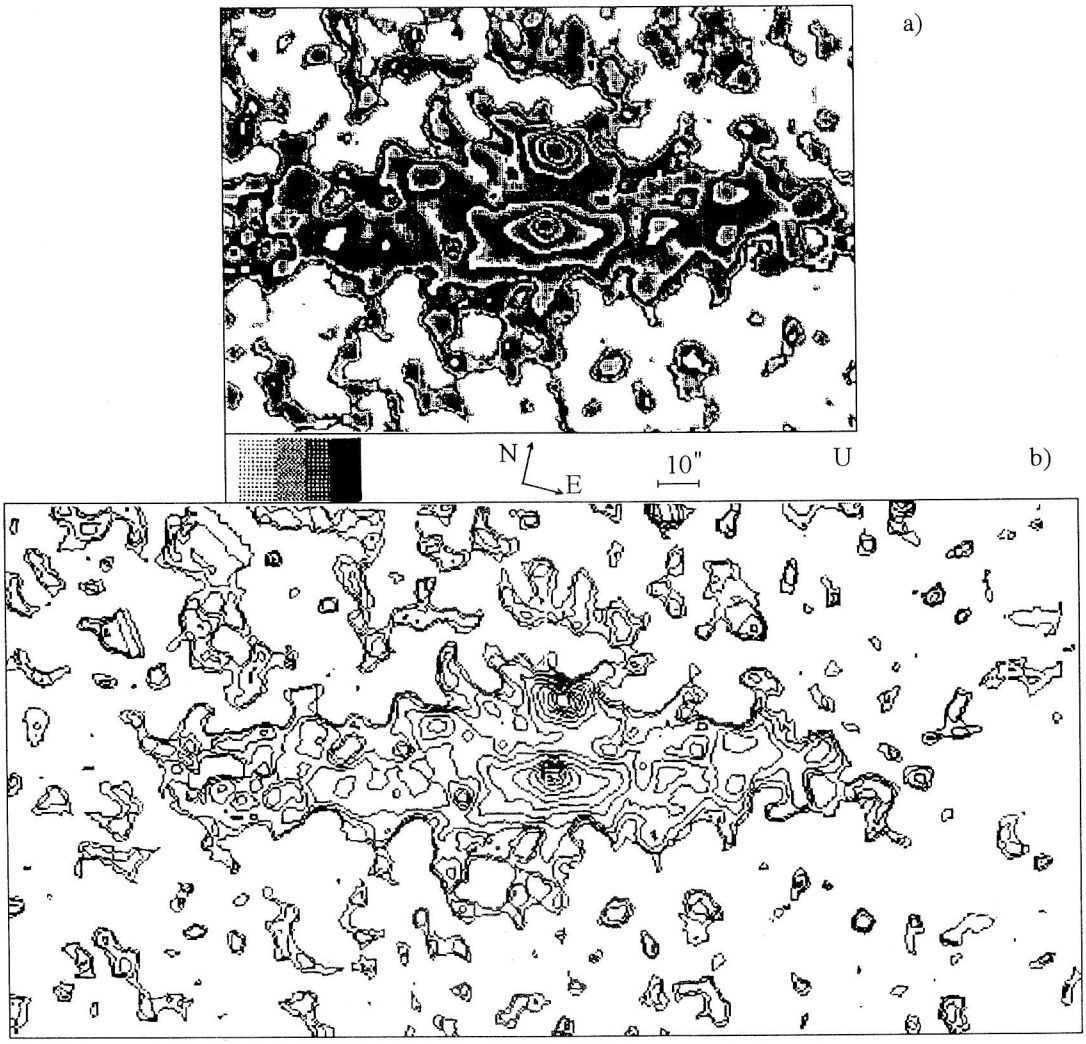

Figure 2: *a) The half–tone maps in the U, B, V filters deduced with* 26 *mag arcsec*$^{-2}$*; at the lower left is th scale of half–tone gradations with a step of* $0\overset{m}{.}2$. *b) The isophote maps in the UBV filters with an interval o* $0\overset{m}{.}5$.

the distribution of radiating matter in the galaxy, its stellar population, star–formation regions, structure of the system. The frames are oriented along the major axis of the galaxy (P.A.=75°). The frames of isophote and isocolour maps have sizes 261 × 130. They cover almost all the galaxy except for the outermost very faint ends of the external arms along the major axis, which are left beyond the frame. The half–tone maps cover the region of the brightest spiral structure (141″ × 102″). The distance between each turn of the spirals increases on a logarithmic scale. The amplitude of the spiral pattern changes little with increasing distance from the center and is superimposed on the exponentially diminishing disk in tensity. At large distances ($R > 100''$) the disk inten sity drops below 27 *mag arcsec*$^{-2}$, and at these dis tances only the spiral arms can be distinguished. Th U brightness profile traces most clearly the crests o the spiral arms where they are intersected by the ma jor axis, in the B and V the brightness profiles ar more smoothed (Fig.6a). The spiral arms in the U band have a higher intensity than in B,V, and thei colours correspond to emission of young blue stars. A distances from 25″ to 65″, where the spiral structur is most developed, the U brightness profile appear flat up to 24 *mag arcsec*$^{-2}$. In Fig.1 one can read

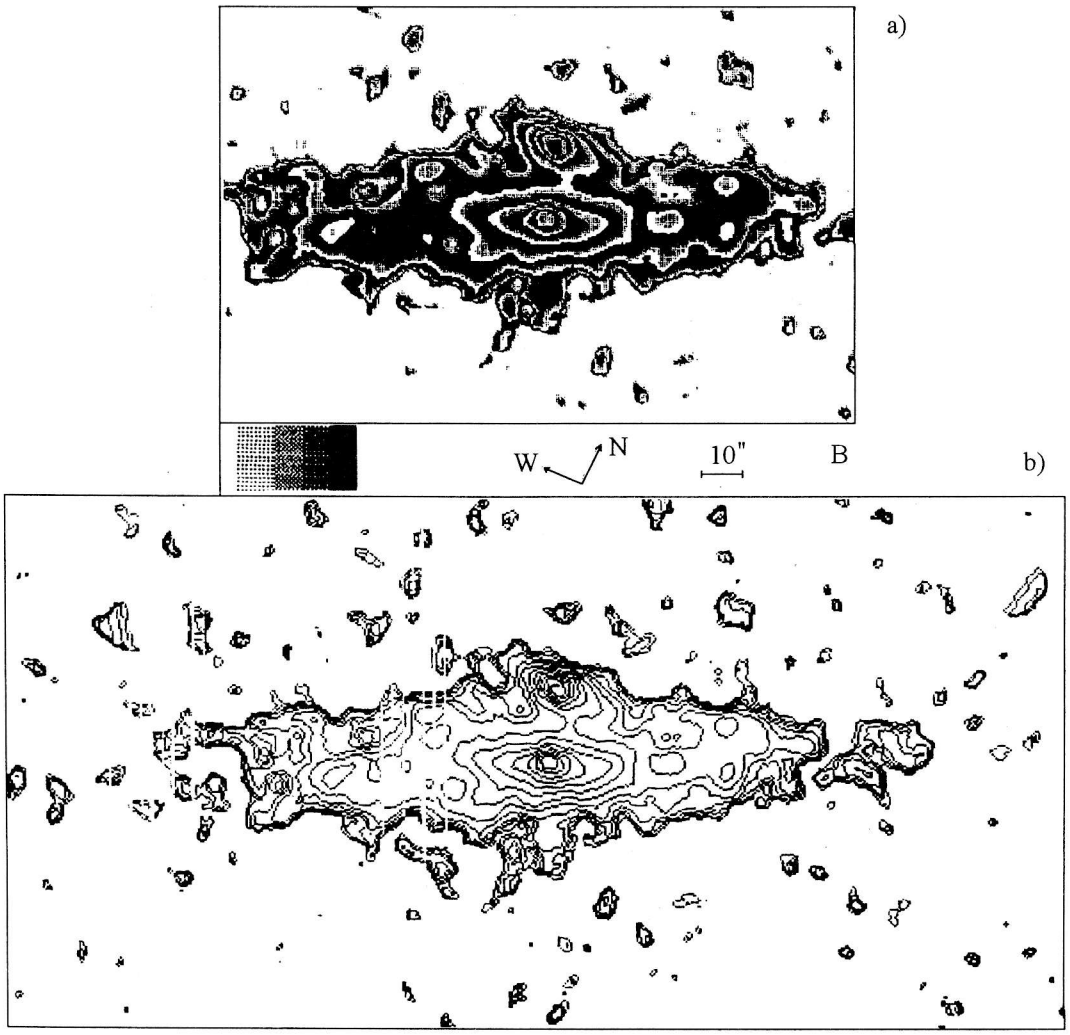

Figure 3: *Designations are as in Fig.2*

ily trace the double–arm spiral structure of the thin arms with bright condensations. On the half–tone and isocolour maps (Figs.2–5) one can easily trace the knots, but the spiral arms themselves are too faint, of low contrast and hardly discernible. However, the very heavily structural isophotes at distances larger than 20″ from the centre along the major axis suggest the presence of spiral arms with a lot of knots. On the isophote and isocolour maps the central lens is well pronounced. Its isophotes are most regular and least compressed, $b/a > 0.36$, up to its boundary. The edges of the lens on the line of nodes at $R = 25''$ coincide with the local minimum on the rotation curve. The local maximum at $R = 15''$ coincides with a certain rise of brightness in the U profile. It is here that Afanasiev (1990) has noted the presence of the brightest emission details of H_α. As a whole the lens is very red, its colour indices B–V=$1\overset{m}{.}1$, U–B=$0\overset{m}{.}35$ except for the central region ($R < 4''$), where the colour indices drop to $0\overset{m}{.}65$ and $-0\overset{m}{.}1$, respectively.

On the U–B isocolour map (Fig.5a) a red long detail, which is located parallel to the major axis at $R \approx 9''$ north of the nucleus, is especially pronounced in the central body; its U–B amounts to $0\overset{m}{.}9$. Its position coincides with two powerful dust lanes which are fairly seen on the photograph. The local maxima in the distribution of U–B, as can be seen in the figures, traces clearly the presence of dust.

The distribution of U,B,V brightnesses and U–B, B–V colours is markedly asymmetrical. In the northern direction the isophotes are closer to each other, than in the southern direction. The decrease in brightness in the southern half of the profiles is more quiet, the colour is bluer than in the northern part of

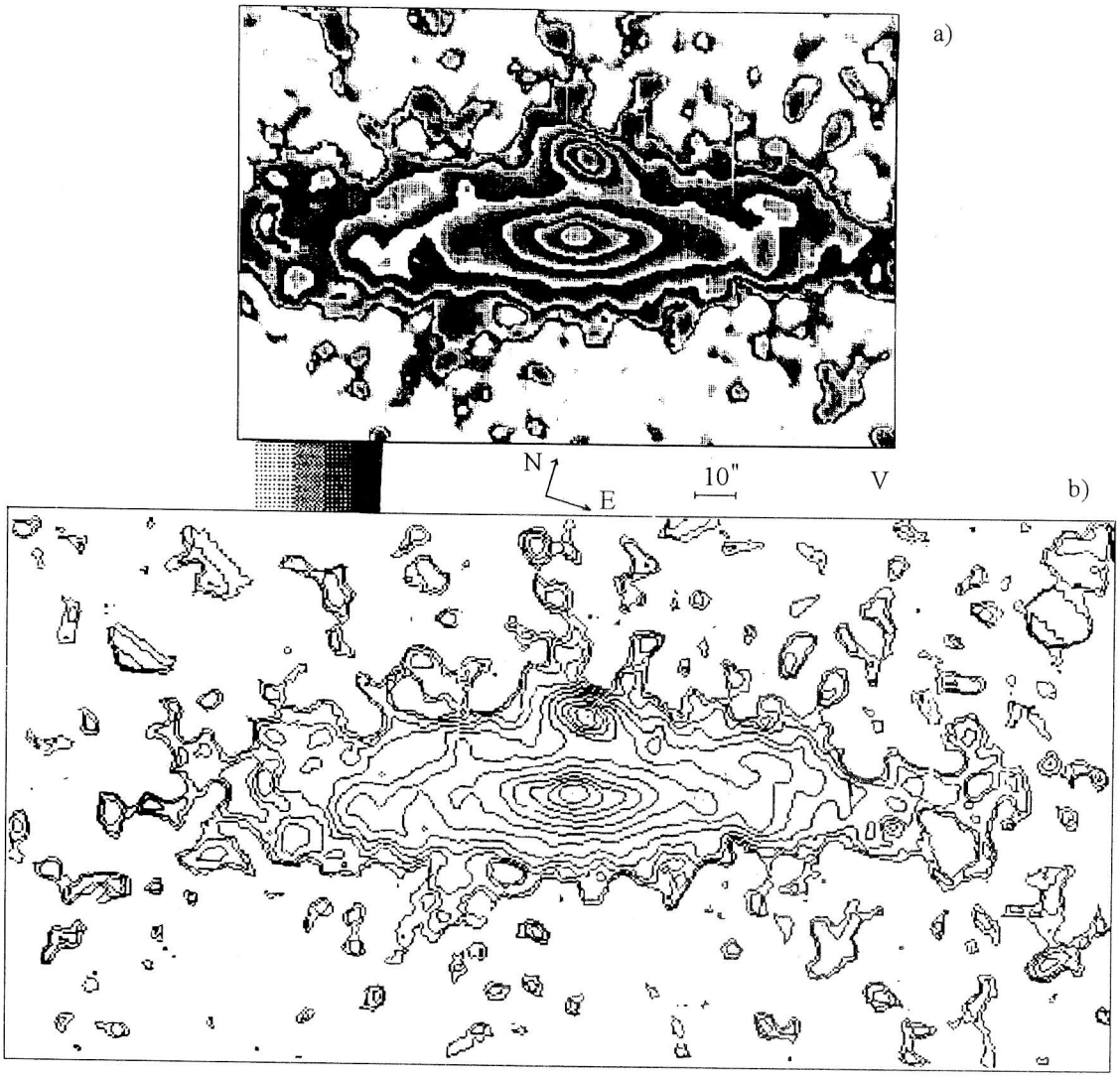

Figure 4: *designations are as in Fig.2*

the galaxy. The south–west side of the companion is also bluer than the north–east. If the conception that dust is located on the inner side of the spiral arms is accepted, a conclusion should then be drawn that the southern parts of Mkn 1040 and of the companion are closer to us. This is confirmed indirectly by the small asymmetry in the brightness distribution along the major axis (Fig.6a). At the same distances from the centre in the region of spirals the eastern side of the galaxy is somewhat brighter than the western. According to Amram et al. (1992) the eastern side is receding from us, and we see the reverse side of the spiral arms; the dust lane is situated behind the galaxy and does not screen radiation of the stars in the spiral arm. As for the western side, it is approaching, and the arms present to us their inner side. The dust lane is in front of the stars of the spiral arm and weakens the light coming from them. According to these considerations the spiral arms are the leadings and the southern side of Mkn 1040 is closer to us.

As has been noted above, the spiral arms are very blue and in the outer regions, at $R > 80''$, where the disk contribution is small, they determine the colour. That is why on the isocolour U–B map (Fig 5a) the galaxy looks considerably smaller since the outer arms melt into the background and are invisible. On the whole some colour gradient can be seen outside the lens, the galaxy becomes bluer towards the edge, which is typical of spiral systems. The contribution of young blue stars grows with distance from the centre, it is maximum in the region of the brightest spiral arms. At larger distances their contribution decreases, and the galaxy reddens again.

The companion galaxy, which is located north of

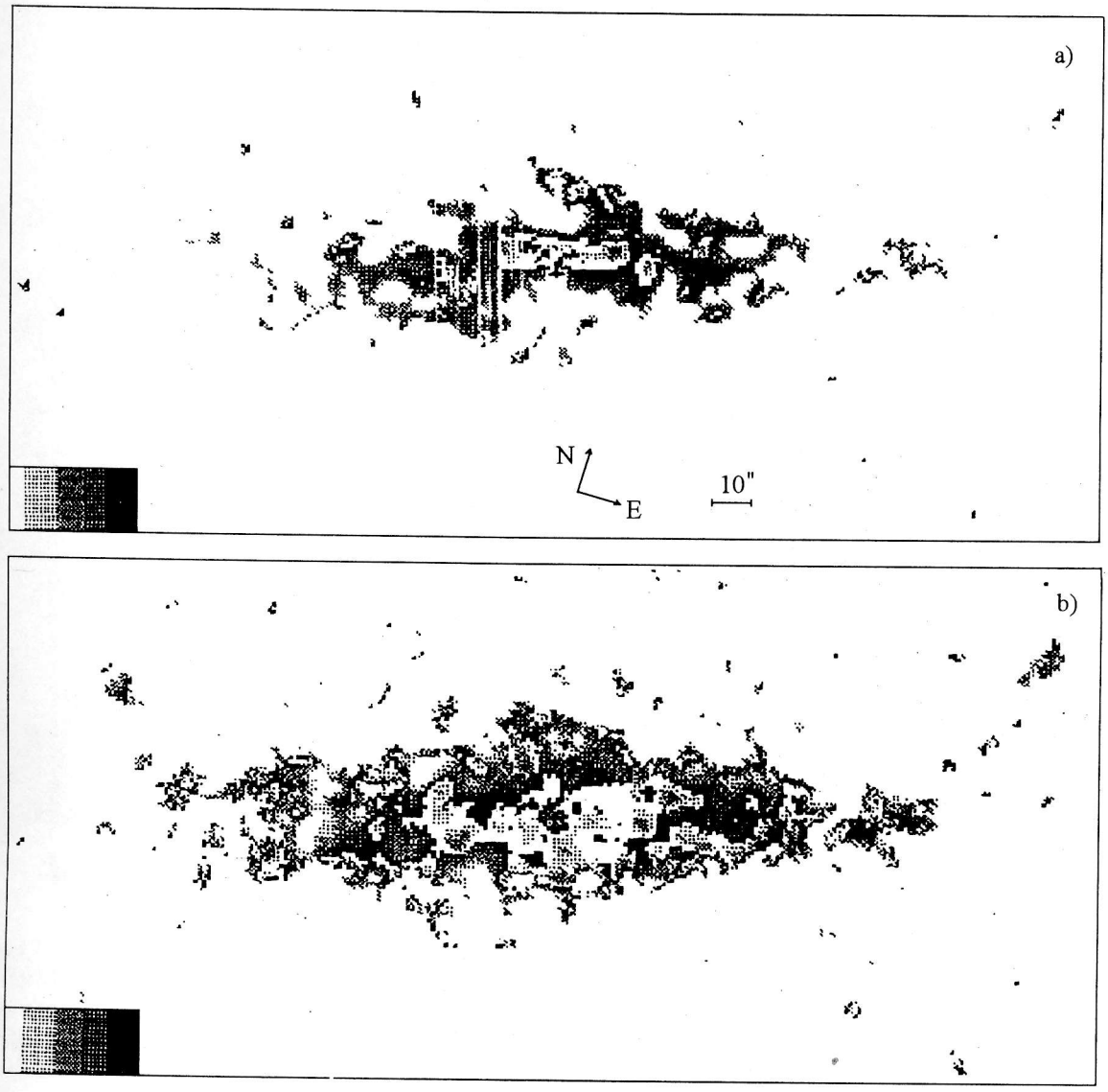

Figure 5: *Isophote a) U–B; at the lower left is the scale of half–tone gradations in the interval from* -0^m.5 *to* 0^m.5 *with a step of* 0^m.2*; b) B–V; at the lower left is the scale of half–tone gradations in the interval from* 0^m *to* 1^m *with a step of* 0^m.2.

the nucleus, is considerably bluer than Mkn 1040. After subtracting the background radiation its integral magnitude and the colours correspond to $B = 16^m.10$, U–B=–0^m.19, B–V=0^m.76. Between the galaxies at the level of isophotes (in magnitudes per square second), 23.6 in U, 23.0 in B, 22.5 in V, a luminous bridge is seen. The companion isophotes are distorted by tidal interaction. Its velocity (Ward and Wilson, 1978) is by 160 km/s greater than in Mkn 1040. In the spectrum taken with the slit aligned along the line that connects the centres of the galaxies emission lines are observed throughout the whole body of the companion. In the U filter the companion looks more round, its isophotes are considerably more rarefied towards the Seyfert nucleus of Mkn 1040 than in the opposite direction. The strong extended emission lines and the unusually blue colour allow us to assume in it a star formation burst initiated by tidal interaction.

4.2. Morphological functions

The most important objective of surface photometry of galaxies is the representation and quantitative analysis of distribution of luminous matter in a system to determine its global parameters from bright-

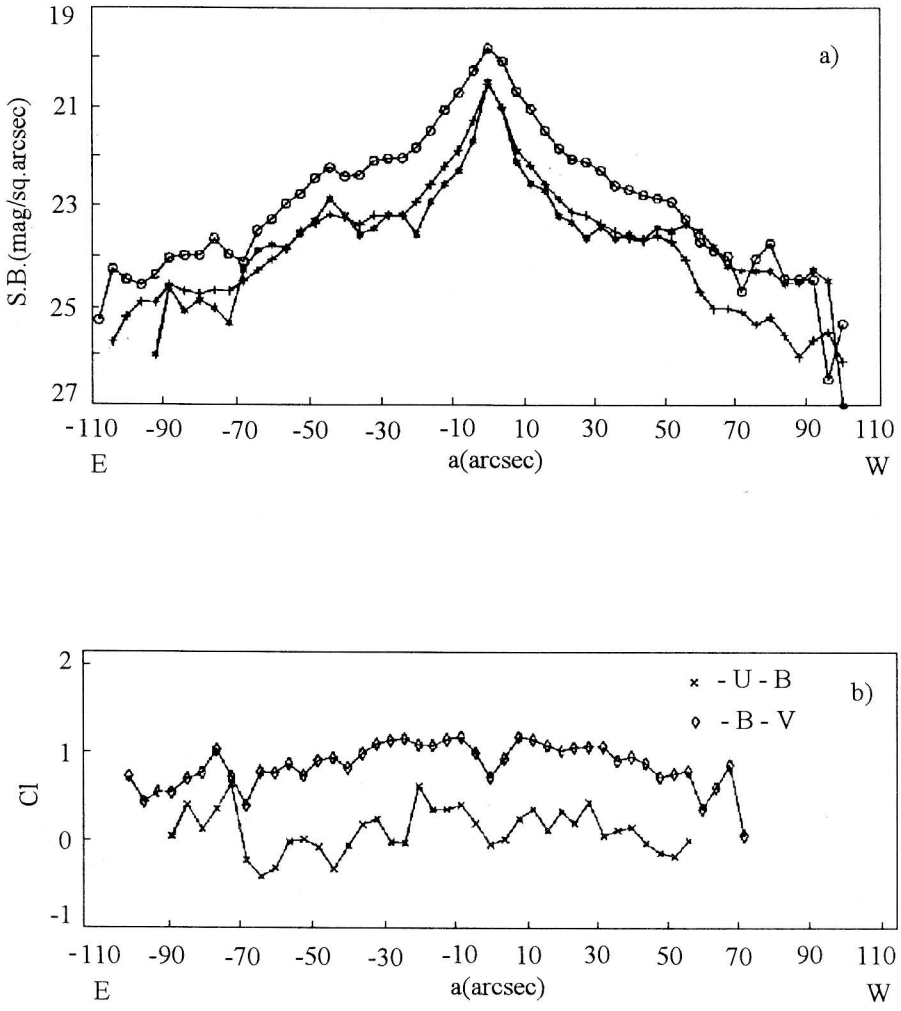

Figure 6: *The distribution of: a) U, B, V brightnesses; b) U-B, B-V colour indices along the major ax (designations are as in Fig.7).*

ness profiles. Both the brightness profiles along the major and minor axes and the generalized brightness profiles obtained by different methods are used. The former are good when describing local inhomogeneities in the distribution of matter, but these particular details involve difficulties in having a general picture. The generalized profiles are obtained by different ways: azimuthal profiles by means of azimuth averaging along the ellipse of equal intensity; equivalent profiles for a given isophote are represented by the radius of a circle of the same area; elliptical profiles, where a given isophote is represented by the fitting ellipse, using the least–squares method. Each of these methods has advantages and disadvantages. The azimuth profiles are convenient for studying the spiral structure of face–on galaxies but inapplicable to strongly compressed systems. The equivalent profiles are good for statistical study of systems of different kinds. However, in this case a lot of informatio about an individual galaxy is lost. The elliptical pr files seem the most universal, and it is easy to chan from these to equivalent ones. We have used the e liptical profiles obtained by Stobie's method (Stobi 1980), which is described in detail in the paper b Georgiev (1990). The whole brightness volume of th image was divided into layers with a specific interv either by brightness, $0.1\,mag\,arcsec^{-2}$, or by AMD densities every $0.1D$. For each layer confined by tw isophote levels its basic parameters were calculate with the help of the method of moments: semi–maj and semi–minor axes a and b, equivalent radius r position angle of the major axis P.A., axis ratio (b/a etc. The weighted mean of the two isophotes, lin iting each layer with allowance for their areas, w taken as the value of isophote brightness for the give layer. The method of moments is very sensitive to i

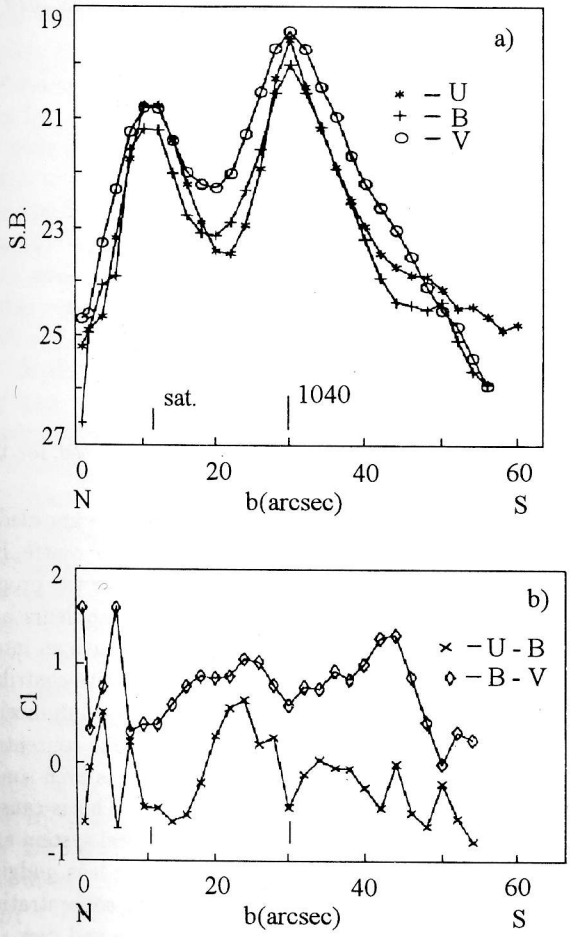

Figure 7: *The distribution of: a) U, B, V brightnesses in Mkn 1040 and its companion along the minor axis: the vertical bars indicate features of the Sy G nucleus (1040) and (sat) its companion; b) U–B, B–V colour indices along the minor axis.*

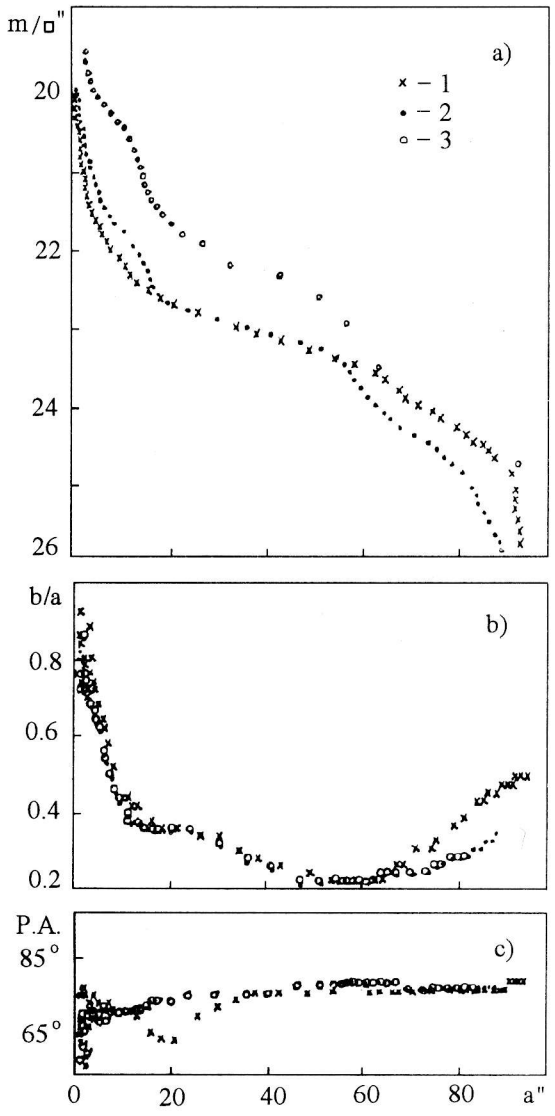

Figure 8: *Morphological functions: a) - elliptical general brightness profile, b) - axis ratio run, c) - the run of position angle of isophotes along the major axis. Designations: crosses - U; filled circles - B, open circles - V.*

terferences of various kinds. That is why the image was thoroughly cleared from background stars and galaxies to obtain reliable results. For this purpose a list of coordinates and radii, or values of ellipses of bright background objects was preliminarily drawn up. Then, using a special program a plane of the local background around a background object was drawn, and the values of the local background plane were substituted for the brightness values. Only after such cosmetic cleaning of the galaxy image its morphological functions were constructed: elliptical brightness profiles, behaviour of the axis ratio and turn of isophotes with respect to the frame alignment along the major axis (Fig.8). The position angle of a given isophote was measured from the main frame direction. The trend of the position angle and axis ratio fairly traces different subsystems of the galaxy, therefore their analysis is extremely helpful for revealing faint global structures of the galaxy.

The chaotic behaviour of the P.A. (Fig.8c) and axis ratio (Fig.8b) near the centre refers to the nuclear region. The transition to their ordered behaviour coincides with the first local minimum on the rotation curve at R = 4″ (Fig.9b). After that, in the region of the lens the axis ratio is rather constant, about $b/a = 0.38$. In the region of the bright spiral structure the isophotes have the largest elongation, which decreases again at the periphery. The position angles of the isophotes remain mainly unchanged except for the U isophotes in the lens region. The latter allows

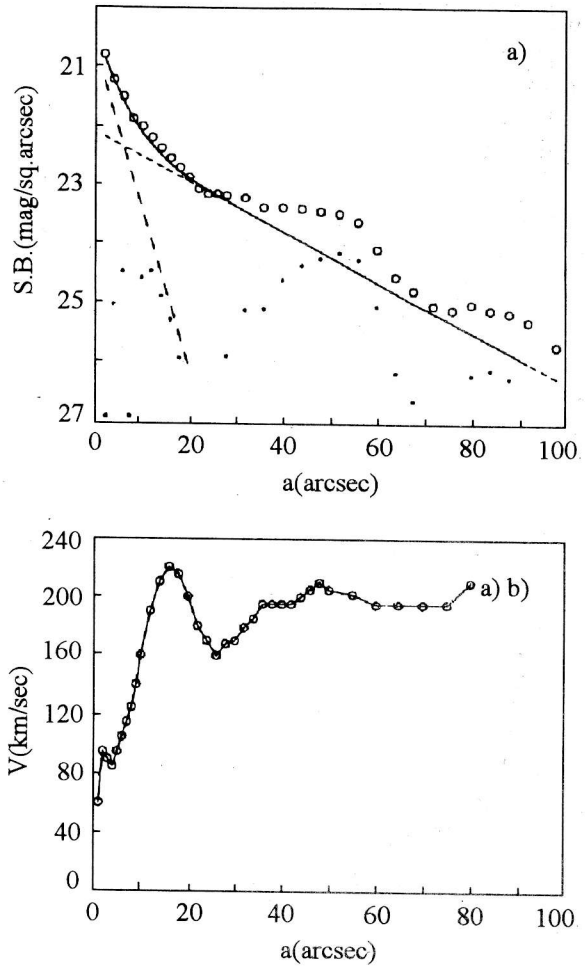

Figure 9: *a) Model division of the general brightness profile of Mkn 1040 into components. Circles - observed profile, straight dashed lines: long dashes - inner steep disk D1 which approximates the lens; short dashes - standard outer disk D0; solid line - total radiation of the two disks; dots - residual radiation, the contribution of the spiral arms; b) curve of rotation of Mkn 1040 taken from Amram et al. (1992).*

us to suspect in it the presence of a faint, blue, extended formation which affects the behaviour of the position angle of the central U isophotes.

On the basis of the morphological functions different morphological parameters of the galaxies were determined: integral asymptotic magnitudes m and equivalent radii r^*, effective equivalent radii r_e^* and effective surface brightnesses μ_e ($mag\ arcsec^{-2}$), mean effective surface brightnesses $\bar{\mu}_e$ ($mag\ arcsec^{-2}$), Vaucouleurs concentration indices $c_{21} = r_e^*/r_{0.25}^*, c_{32} = r_{0.75}^*/r_e^*, c_{31} = r_{0.75}^*/r_{0.25}^*$, concentration parameters c (Kent, 1985), and absolute magnitudes of the host galaxy, M(h.G.). These data are presented in Table 1. Corrections for the proper absorption were not introduced, all the values were only corrected for the absorption in the Galaxy.

Table 1: *Photometrical parameters of Mkn 1040*

Phot.param.	U	B	V
m	13.98	13.65	12.88
$r^* kpc$	17.15	19.67	19.45
$r_e^* kpc$	13.74	9.97	8.68
μ_e	24.28	23.75	22.86
$\bar{\mu}_e$	23.81	23.12	22.04
c_{21}	2.34	2.02	2.37
c_{32}	1.43	1.48	1.55
c_{31}	3.36	2.88	3.68
c	3.80	3.15	3.57
$M(h.G.)$	-20.19	-20.58	-21.32

Usually all concentration indices give a knowledge on the degree of concentration towards the centre. For the proper disk $c_{21} = 1.75$, $c_{32} = 1.61$; for the proper bulge $c_{21} = 2.74$, $c_{32} = 2.55$ (De Vaucouleurs and Aguero, 1973); for spiral galaxies they have an intermediate value which depends on the relative contribution of the bulge and disk to the integral luminosity. Dust reduces their value. The values of the concentration indices c_{32} in Mkn 1040 (Table 1) is even somewhat smaller than for the proper disk. This is caused by the great amount of dust in the spiral system and low concentration of the disk. The inner lens, judging by the value c_{21} (Table 1), occupies by concentration an intermediate position between bulge and disk.

4.3. Analysis of brightness profiles. Decomposition into components

The most important problem of surface photometry is representation and quantitative analysis of distribution of luminous matter in a galaxy for determining its global structures and their relative significance. A multicomponent analysis of basic parameters of galaxies has shown that the relationship between the disk and spherical components is most frequently responsible for the variety of properties of galaxies (Watanabe et al., 1985). Analysing the systematic bulge–to–disk ratio, Simien and de Vaucouleurs (1986) have found that the best indicator of the system's state is the relative magnitude of the bulge since its parameters vary over a very wide range, while the disk parameters change in a rather limited range. However, only in half of the galaxies studied photometrically the brightness profiles are liable to standard decomposition into spherical and disk components. The brightness profiles of Mkn 1040 belong to type II by Freeman (1970). Profiles of this type are most difficult to decompose. The complicated spiral structure and numerous dust lanes make the profile complex and smear the general picture.

On the brightness profiles parallel to the minor axis, where the contribution of the outer disk is negligibly small, one can try to examine the brightness behaviour in the spherical component. As is seen in Fig.7a, on the southern side of this profile, which is undistorted by the companion, the brightness behaviour in U,B,V obeys an exponential law. Along the small axis b the inclination of the profiles is approximately equal in all three spectral bands with a disk scale length $\alpha^{-1} = 4''.5$ (1.43 kpc). Only in the outer region at $b > 24''$ the contribution of the outer disk and spiral arms in the U and B is noticeable.

Analysing the general B profile along the major axis, we attempted to find acceptable decomposition within the framework of a standard model. The fitting by two exponential disks $D1 : B(0)_1 = 20.7\, mag\, arcsec^{-2}, \alpha^{-1} = 1.27 kpc; D0 : B(0) = 22.1\, mag\, arcsec^{-2}, \alpha^{-1} = 8.16 kpc$ turned out most successful. The obtained brightness distribution and the model details are presented in Fig.9a. It describes well the observed profile. The central points ($a < 4''$), were omitted since the photometry is not confident here. After the correction for the proper and galactic absorption and for the inclination effect the following surface brightnesses of the disks were obtained: $B(0)_c = 19.9\, mag\, arcsec^{-2}, I(0)_c = 679 I_\odot pc^{-2}$ for $D1; B(0)_c = 21.36\, mag\, arcsec^{-2}, I(0)_c = 177 I_\odot pc^{-2}$ for $D0$. With these parameters the luminosities of the disks calculated by the formula $L_D = 2\pi\alpha^{-1}$ are $L_{D1} = 7.97 \cdot 10^9 L_\odot, L_{D0} = 7.40 \cdot 10^{10} L_\odot, D1/D0 = 0.1, L_{D1+D0} = 8.2 \cdot 10^{10} L_\odot$.

The residual luminosity distribution (Fig.9a) points out plainly to the spiral structure. The total luminosity of the spiral arms is $L_S = 2 \cdot 10^9 L_\odot$, which amounts to 2% of the total luminosity of the galaxy.

Note the distinct boundary between lens and disk (Figs.6a, 9a). It coincides with the local minimum on the rotation curve (Fig.9b). Probably the character of rotation in the central part is chiefly defined by the central disk $D1$.

Let us estimate the mass of the central lens, which is determined from the local maximum, and the mass of the whole galaxy from the velocity of getting to the plateau by the formula: $M(R) = 2.32 \cdot 10^5 RV^2(R)$. The rotation curve is traced up to $80''$ without signs of fall. The natural boundary of the disk, as can be seen from Fig.6, is located at $R = 100''$ (31.8 kpc). Then the mass of the galaxy is equal to $M_T = 32.5 \cdot 10^{10} M_\odot$, while the mass of the central disk $D1$ is $M_1 = 5.42 \cdot 10^{10} M_\odot$. Using these values, we determined $M_T/L_T = 3.97$ and $M_1/L_1 = 6.8$. The extended disk $D0$ accounts, apparently, for the greater part of the mass. We have estimated the central density of this disk ρ_0 and its mass by the formula $M_D = 2\pi\rho_0\alpha^{-2} : \rho_0 = 701 M_\odot/pc^2, M_{D0} = 2.9 \cdot 10^{11} M_\odot$.

From a comparison between the rotation curve and photometric model it is clear that at the point of the local minimum the radial velocity function has a discontinuity. The inner region, accelerating its motion, is pressed, and the gas from the inner side with respect to the break point streams to the centre. On the other side from the break point deceleration and gas outflow occur. That is why at the local minimum point rarefaction arises and a certain deficit of surface brightness must be present, which is observed in our case.

The authors are thankful to V.L. Afanasiev for the helpful discussions.

The work has been done under financial support of the Russian Inter-high-school program "Astronomiya" The work of one of the authors (Ts.B. Georgiev) is particularly supported by the grant F–342/93 of the Bulgarian Ministry of Education and Science.

References

Adams T.F.: 1977, Astrophys. J. Suppl. Ser., **33**, 19.
Afanasiev V.L.: 1981, Pis'ma Astron. Zh., **7**, 390.
Afanasiev V.L.: 1990, Thesis, 92, (in Russian).
Amram P., Marcelin M., Bonnarel F., Boulesteix J., Afanasiev V.L., Dodonov S.N.: 1992, Astron. Astrophys., **263**, 69.
Dahari O., de Robertis M.M.: 1988, Astrophys. J. Suppl. Ser., **67**, 249.
De Vaucouleurs G., Aguero E.: 1973, Publ. Astr. Soc. Pacific, **85**, 150.
Freeman K.C.: 1970, Astrophys. J., **160**, 811.
Georgiev Ts.B.: 1990, Astrofiz. Issled. (Izv. SAO), **30**, 111.
Kent S.M.: 1985, Astrophys. J. Suppl. Ser., **59**, 115.
Kotilainen J.K., Ward M.J., Williger G.M.: 1993, ESO, preprint, No.908.
Lipovetskij V.A., Neizvestny S.I., Neizvestnaya O.M.: 1987, Soobshch. Spets. Astrofiz. Obs., **55**, 3.
MacKenty J.W.: 1990, Astrophys. J. Suppl. Ser., **72**, 231.
Malkan M.A., Margon B., Chanan G.A.: 1984, Astrophys. J., **280**, 66.
Metik L.P., Pronik I.I.: 1981, Astrofizika, **17**, 629.
Neizvestny S.I.: 1986, Soobshch. Spets. Astrofiz. Obs., **51**, 5.
Pavlova N.N.: 1981, Morphological analysis of Sy galaxies, dep. manuscript, No. 1236, (in Russian).
Rafanelli P., Schulz H.: 1983, Astron. Astrophys., **117**, 109.
Richter G.M.: 1978, Astron. Nachr., **299**, 283.
Richter G.M., Lorenz X.: 1989, User's instruction.
Simien F., de Vaucouleurs G.: 1986, Astrophys. J., **302**, 564.
Simkin S.M., Su H.J., Schwarz M.P.: 1980, Astrophys. J., **237**, 404.
Stobie R.: 1980, J.Brit.Interplan.Soc., **33**, 323.
Ward M.J., Wilson A.S.: 1978, Astron. Astrophys., **70**, L79.
Watanabe M., Kodaira K., Okamura S.: 1985, Astrophys. J., **292**, 72.
Xanthopoulos E.,de Robertis M.M.: 1991, Astron. J., **102**, 1980.

Yee H.K.: 1983, Astrophys. J., **272**, 473.

Zasov A.V., Neizvestny S.I.: 1989, Pis'ma Astron. Zh., **7**, 390.